



## RESEARCH ARTICLE

# Biomaterial characterization of off-the-shelf decellularized porcine pericardial tissue for use in prosthetic valvular applications

Joshua A. Choe  | Soumen Jana | Brandon J. Tefft | Ryan S. Hennessy | Jason Go | David Morse | Amir Lerman | Melissa D. Young 

Department of Cardiovascular Diseases, Mayo Clinic, Rochester, MN, USA

**Correspondence**

Melissa D. Young, Division of Cardiovascular Diseases, Mayo Clinic, 200 First Street SW, Rochester, MN 55905, USA.

Email: young.melissa@mayo.edu

**Funding information**

National Institute of Health T32, Grant/Award Number: HL007111; HH Sheikh Hamed bin Zayed Al Nahyan Program in Biological Valve Engineering

**Abstract**

Fixed pericardial tissue is commonly used for commercially available xenograft valve implants, and has proven durability, but lacks the capability to remodel and grow. Decellularized porcine pericardial tissue has the promise to outperform fixed tissue and remodel, but the decellularization process has been shown to damage the collagen structure and reduce mechanical integrity of the tissue. Therefore, a comparison of uniaxial tensile properties was performed on decellularized, decellularized-sterilized, fixed, and native porcine pericardial tissue versus native valve leaflet cusps. The results of non-parametric analysis showed statistically significant differences ( $p < .05$ ) between the stiffness of decellularized versus native pericardium and native cusps as well as fixed tissue, respectively; however, decellularized tissue showed large increases in elastic properties. Porosity testing of the tissues showed no statistical difference between decellularized and decell-sterilized tissue compared with native cusps ( $p > .05$ ). Scanning electron microscopy confirmed that valvular endothelial and interstitial cells colonized the decellularized pericardial surface when seeded and grown for 30 days in static culture. Collagen assays and transmission electron microscopy analysis showed limited reductions in collagen with processing; yet glycosaminoglycan assays showed great reductions in the processed pericardium relative to native cusps. Decellularized pericardium had comparatively low mechanical properties among the groups studied; yet the stiffness was comparatively similar to the native cusps and demonstrated a lack of cytotoxicity. Suture retention, accelerated wear, and hydrodynamic testing of prototype decellularized and decell-sterilized valves showed positive functionality. Sterilized tissue could mimic valvular mechanical environment in vitro, therefore making it a viable potential candidate for off-the-shelf tissue-engineered valvular applications.

**KEYWORDS**

biomechanics, decellularization, heart valves, pericardial tissue, sterilization, tissue engineering

This is an open access article under the terms of the Creative Commons Attribution-NonCommercial-NoDerivs License, which permits use and distribution in any medium, provided the original work is properly cited, the use is non-commercial and no modifications or adaptations are made.

© 2018 The Authors Journal of Tissue Engineering and Regenerative Medicine Published by John Wiley & Sons Ltd

## 1 | INTRODUCTION

Valvular heart disease (VHD), which can present through aortic stenosis, is a critical condition that may compromise valvular structure and function resulting in increased morbidity and mortality. In the United States today, the overall prevalence of VHD is 2.5% with up to 13.3% of those over the age of 75 (d'Arcy, Prendergast, Chambers, Ray, & Bridgewater, 2011). Currently, the gold standard treatment for aortic localized VHD is valvular replacement; however, current valve substitutes have severe limitations for universal application (Walther, Blumenstein, van Linden, & Kempfert, 2012).

Despite the extensive clinical usage of current valve replacements, both mechanical and glutaraldehyde (GA)-fixed bioprostheses are similarly limited in long-term and paediatric application as they lack viability in terms of remodelling, repair, and growth. These constructs are accompanied by adverse consequences, such as necessity of taking life-long anticoagulants, or increased risk of calcification and progressive degradation, respectively (Jang et al., 2012; Walther et al., 2012). Thus, crafting of heart valves from viable explant tissues has been explored.

Decellularized xenograft tissues are suitable for transplant purposes as they allow for extracellular matrix (ECM) preservation and can allow for restoration of tissue viability and function through recellularization (Crapo, Gilbert, & Badylak, 2011). Refinement of decellularization techniques, by utilization of anionic detergents, such as sodium dodecyl sulfate (SDS), in low concentrations, appear to retain more glycosaminoglycans (GAGs) and stress-strain properties compared with other agents (Mendoza-Novelo et al., 2011; Steinhoff et al., 2000; Wilson, Courtman, Klement, Lee, & Yeager, 1995). Although there have been great limitations in the utilization of decellularized whole heart valves, (Kasimir et al., 2006; Simon et al., 2003; Voges et al., 2013) mostly due to previously unforeseen immune responses to epitopes like galactose- $\alpha$ -1,3-galactose ( $\alpha$ -gal), the utilization of other starter materials may have potential for future application. Pericardial tissue is extensively used as a versatile biomaterial replacement for native tissues (Schmidt & Baier, 2000), including valves, as it is anisotropic, (Gauvin et al., 2012; Labrosse, Jafar, Ngu, & Boodhwani, 2016) easy to manipulate, and shows greater durability *in vivo* compared with porcine-fixed valves (Grunkemeier, Furnary, Wu, Wang, & Starr, 2012).

Previous studies have investigated the impact of decellularization and GA fixation on the mechanical properties of bovine pericardium (Bourguine, Pippenger, Todorov, Tchang, & Martin, 2013; Mendoza-Novelo et al., 2011). However, decellularized bovine pericardial tissue has been shown to be limited in resilience when used for valve creation, possibly due to insufficient mechanical properties (Braga-Vilela, Pimentel, Marangoni, Toyama, & de Campos Vidal, 2008). Because valves are functionally elastic tissues and stiffening can negatively impact the phenotype of valvular interstitial cells (VICs), replacement biomaterials should have similar qualities (Butcher, Simmons, & Warnock, 2008; Thubrikar, Piepgrass, Boshier, & Nolan, 1980).

Many studies have looked at the mechanics of bovine pericardium (Mendoza-Novelo et al., 2011); yet porcine pericardial tissue, which is structurally more similar to human tissue, could be a better biomaterial for tissue engineering purposes (Fentie, Allen, Schenck, & Didio,

1986). For instance, porcine, compared with bovine, pericardium is similar in collagen structure and organization (Gauvin et al., 2012); however, porcine pericardium is thinner, which may increase efficiency of decellularization process in regard to removal of xenogeneic materials (Fentie et al., 1986).

In bovine pericardium, decellularization has allowed for decreases in the elastic modulus relative to GA treatment (Hulsmann et al., 2012). Porcine pericardium, while demonstrating lower peak tensile stress than bovine pericardium, is an intrinsically less stiff material and could show even further reductions in stiffness with decellularization (Gauvin et al., 2012; Hasan et al., 2014). Furthermore, religious and cultural practices may limit the clinical usage of explant tissues. For instance, one patient may accept the use of a bovine but not porcine bioprosthetic or vice versa. Therefore, it has been vital to characterize porcine tissues, as bovine tissues have previously been described, in order to best fit the needs of patients (Easterbrook & Maddern, 2008).

At present, no study has compared the impact of tissue processing on the direction-specific properties of decellularized and sterilized porcine pericardium. Most tissue-engineered valves under development require biomaterial harvesting or creation, *in vitro* augmentation and synthesis of the valve, and potentially bioreactor preconditioning before implantation *in vivo*. However, sterile handling and the time of current (TEHV) Tissue Engineered Heart Valve production are not optimal for fabrication and clinical application, respectively. Not only is working aseptically difficult with the manufacturing of a complex device such as a decellularized valve, but it is veritably impossible. The development of an off-the-shelf valve that could be sterilized and packaged prior to implantation would be highly desirable for fabrication commercialization purposes. Such sterile valves could then be seeded and preconditioned *in vitro* or implanted directly. Supercritical CO<sub>2</sub> (sCO<sub>2</sub>) has been shown to be useful in the sterilization of fragile biomaterials, and previously, this laboratory has had success in sterilizing whole porcine valves without reductions of mechanical integrity (Bernhardt et al., 2015; Hennessy et al., 2017).

In the current study, the impact of various treatment conditions on uniaxial loading was assessed in porcine pericardium and was contrasted to both native pericardium and native valvular cusps. Furthermore, the impact of processing on matrix structure and function was evaluated through scanning electron microscopy (SEM), transmission electron microscopy (TEM), histology, and cytotoxicity testing. We postulated that native pericardial tissue would exhibit the greatest mechanical properties (ultimate tensile strength [UTS] and stiffness); however, we hypothesized that the process of decellularization, as well as sterilization, could produce tissues that are better representative of the mechanical properties of native valvular tissue. Furthermore, characterization of sterilized tissues allows for the potential to develop an off-the-shelf tissue-engineered aortic heart valve.

## 2 | METHODS

### 2.1 | Tissue collection and preparation

In this study, five groups ( $n = 24$  each) were tested, including three pericardial processing conditions and both native valvular and

pericardial tissues. Whole porcine hearts were acquired and randomly selected from a local abattoir (Hormel Food Corp., Austin, MN, USA). Pericardial sacs were extracted and cleaned down to remove non-fibrous components, and aortic leaflets were dissected. Following cleaning, pericardial tissue were then randomly subjected to one of three processing conditions: decellularization, fixation, or decellularization followed by sterilization (decell-sterilized). Native pericardium and valvular cusps were kept intact for comparison.

Pericardial tissue specimens ( $n = 48$ ) were decellularized with low concentration 0.5%–1% (wt/vol) SDS (Thermo Fischer Scientific, Waltham, MA) in diH<sub>2</sub>O and 0.02% (wt/vol) DNASE grade II (DNASE 1, Sigma-Aldrich, St. Louis, MO) for 2 days. The tissue was then washed with a 1 M Tris buffered DNASE solution (Bio-Rad, Hercules, CA) for 12 hr and then washed in phosphate-buffered saline (PBS) for 14 days to remove residual chemicals. Following decellularization, half of the samples ( $n = 24$ ) underwent sCO<sub>2</sub> sterilization through a commercial entity (NovaSterilis, Inc., Lansing, NY, USA) as previously reported (Hennessy et al., 2017). Additional pericardial tissue specimens ( $n = 24$ ) were fixed in 1.25% (vol/vol) GA solution in PBS for a minimum of 24 hr. Fixed tissue was then stored in a solution of 0.25% (vol/vol) GA and PBS. Fixed and decellularized tissues were tested within 24 hr of process completion. Native valvular and pericardial tissues were subject to testing immediately after collection.

## 2.2 | Tensile mechanical testing

Following processing, mechanical testing was performed per ASTM F2150-13 ASTM F2150-13. (n.d.) to analyse treatment effects in contrast to native tissues. To evaluate anisotropy, the specimens were viewed with a light box, and then, specimens were cut in different directions, half of each treatment group was subjected to circumferential (Circ.) and the other half to longitudinal (Long.) tensile testing ( $n = 12$  for each direction and  $n = 24$  for each processing group). A razor blade punch was used to section  $14.5 \times 4.5$  mm ( $l \times w$ ) pieces from the pericardial tissue processed from each condition. Collagen fibres were positioned across the long and short axis of the punch, respectively. Positioned at the centre of each sample, digital calipers (Mitutoyo America Corp., Aurora, IL, USA) were utilized to assess the thickness of the tissue. Custom grips were clamped onto each respective sample and attached to a tensile testing device via sandpaper and cyanoacrylate adhesive. The tensile properties were evaluated using a tensile testing machine (ElectroForce 3200, Bose Corporation, Eden Prairie, MN, USA) equipped with a 5-lb load cell, operating at an extension rate of 0.1667 mm/s, and with a preload of 0.01 N. Tissue samples were preconditioned by loading and unloading under a constant rate of 60 N/m, similar to the physiologic loading of aortic leaflets (Martin & Sun, 2012), and it was repeated for 10 cycles until the stress-strain loop of the sample appeared to be periodic. The samples were tested under ambient temperature and were kept hydrated using normal saline solution throughout testing. Tensile strength, elongation at break, and stiffness were calculated from the load versus displacement data. Elastic modulus was calculated from the slope of the linear region on the stress-strain response curves (second linear region).

## 2.3 | ECM evaluation

In order to probe potential microscopic changes in ECM morphology and structure, SEM, TEM, porosity testing, and histology were performed. Two to three representative micrographs were taken from one sample in each processing condition to qualitatively assess the matrix. Per cent porosity was determined via the liquid displacement method, as previously described, ( $n = 5$  per process condition), where the tissue specimens were placed in a known volume of de-gassed water, and evacuation–repressurization cycles were performed to force the liquid into the pores (Loh & Choong, 2013). Cell content was assayed through DAPI staining. General matrix properties were then assessed through histological staining for haematoxylin and eosin and collagen fibres through picrosirius red and Masson's trichrome staining. Alcian periodic acid–Schiff staining was performed to visualize GAGs.

## 2.4 | Bioassays

Collagen and GAG content analysis was performed on all the tissue specimens. Collagen quantifications of the tissue samples were conducted according to the manufacturer protocol (Sigma, USA). The samples ( $n = 3$  per processing group) were homogenized in 100  $\mu$ l of water and then added to 100  $\mu$ l of 12 N HCl and hydrolyzed at 120 °C for 3 hr. A 50  $\mu$ l of the hydrolyzed sample was placed on a 96-well plate and dried at 60 °C. The samples were incubated at room temperature for 5 min after a 100  $\mu$ l chloramine T/oxidation buffer mixture (94:6) was added. The samples were incubated again at 60 °C for 90 min after 100  $\mu$ l of diluted DAMB reagent was added. Once the samples reached room temperature, their absorbance was measured at 560 nm and compared with the reference curve obtained from hydroxyproline solution. Collagen quantification data were expressed in terms of hydroxyproline. To quantify the GAG content, a GAG assay kit (Blyscan, Biocolor, USA) was utilized following the manufacturer's recommendations. The samples ( $n = 4$  per processing group) were lyophilized and digested in papainase buffer containing papain type III (Worthington Biochemical, USA). Supernatants were collected by centrifugation. The sample was evaluated at 656 nm absorbance and compared with the reference curve using known GAG standard solutions.

## 2.5 | Cell compatibility study and immunogenicity

Leaflets were collected from porcine aortic heart valves and were used for isolation of vascular endothelial cells (VECs) and VICs following the procedure as stated. The leaflets were washed with PBS (Hyclone, USA), then placed in trypsin (Invitrogen, USA) at 37 °C for 5 min. Both sides of each leaflet were then swabbed gently with a cotton swab to remove the endothelial layer from their surfaces. The cotton swab was then dabbed within 0.5% (wt/vol) type I collagenase (Worthington Biochemical, USA) solution in PBS to dislodge the VECs from the swab. Through centrifuging at 1,000 rpm for 10 min, VECs were collected from the cell suspension/collagenase. Collected VECs were then cultured in endothelial cell culture medium (Lonza, USA) supplemented with 10% fetal bovine serum (Atlas Biologicals, USA) and 1% penicillin–streptomycin (Life Technologies, USA) for their expansion. After removal of VECs from the leaflets, the leaflets were digested in 0.5% (wt/vol) type I collagenase solution at 37 °C for 5 hr. Through

centrifuging at 1,000 rpm for 10 min, VICs were isolated from digestion. Isolated VICs were cultured in tissue culture media containing Dulbecco's modified Eagle's medium (Corning, USA) supplemented with 10% fetal bovine serum and 1% penicillin–streptomycin (Life Technologies, USA) for their expansion.

Decellularized, sterilized, and fixed pericardial tissue ( $n = 36$ ) were uniformly cut into sections and seeded with cells to test for potential cytotoxicity incurred from the decell-sterilized processes. Porcine VICs ( $n = 6$ ) and VECs ( $n = 6$ ) were seeded gravimetrically onto each tissue group, for a total of 36 samples. The control group was VICs ( $n = 6$ ) and VECs ( $n = 6$ ) in cultured media for a total of 12 samples. The tissue was placed in a Dulbecco's modified Eagle's medium within wells of a 6-well plate and secured initially with ring. Media changes were conducted every 3 days, and cells were not passaged. SEM evaluation was performed on Day 15 for the decell-sterilized group, and a LIVE/DEAD® assay (ThermoFisher Scientific, Waltham, Massachusetts, USA) was used per manufacturer guidelines on Day 30 to assess VEC viability on all groups. Cells grown in a blank well were utilized as a comparison control.

In order to test the existence of alpha-gal epitope, decellularized, sterilized, and native tissues were stained. Antigen retrieval was performed using steam method in IHC-Tek Epitope Retrieval Solution (IW-1100) for 35 min and then cooled for 20 min. The slides were washed in PBS and blocked with 3% H<sub>2</sub>O<sub>2</sub>. After washing, the slides were incubated in alpha-gal Epitope (Gal $\alpha$ 1-3Gal $\beta$ 1-4GlcNAc-R) monoclonal antibody M86 (Enzo Life Sciences, Farmingdale, NY) at 1:5 dilution with IHC-Tek Antibody Diluent (IHC World, Ellicott City, MD) for 1 hr at room temperature. Afterwards, the slides were incubated with biotinylated Horse Anti-Mouse secondary antibody 1:500 (Vector Lab, Burlingame, Ca) for 30 min, were washed in PBS, and then incubated with HRP-Streptavidin 1:500 (Jackson ImmunoResearch, West Grove, PA). The bound antibody was visualized using DAB (Ellicott City, MD, IHC World, Cat#IW-1600, 0.05% DAB) for 5–10 min. The sections were counterstained, dehydrated, and mounted. Images were captured at 10 $\times$  and 20 $\times$  magnifications using light microscopy.

Enzyme-linked immunosorbent (ELISA) quantification of alpha-gal was performed on decellularized, sterilized, and native tissues via a 96 strip well sandwich ELISA kit purchased from MyBiosource, Inc. (San Diego, CA, product MBS746011). Samples (1.5–3  $\mu$ g of protein extracts) were prepared according to kit manufacturer's suggestion. Intra-assay and inter-assay coefficients of variation values were <10%. The sensitivity of detection in this assay was 0.1 ng/ml. All tests for each sample were performed in duplicate. Relative concentrations of alpha-gal epitopes were calculated on the basis of fresh porcine pericardial defined as 100%.

## 2.6 | Suture retention testing

The suture retention capabilities of processed pericardial tissue was tested following the straight-across procedure per ISO 7198 using a tensile machine. Crosshead speed was set to 100 mm/min. Prolene 5–0 suture was inserted 4 mm from the end of the 4  $\times$  10 mm piece of laser cut tissue and through the tissue to form a half loop. The suture was pulled at the rate of 100 mm/min crosshead speed. Twelve specimens

were tested in each group. The force (g) required to pull the suture through and/or cause the tissue to fail was recorded (ISO 7198, 2016).

## 2.7 | Hydrodynamic testing

Hydrodynamic evaluation was performed in a pulse duplicator to evaluate performance under physiological conditions. Two prototype transcatheter aortic valves were prepared. One valve was made with decellularized, and one was made with decell-sterilized porcine pericardial tissue. The tissue was laser cut into a custom tri-leaf design, then sutured to a custom nitinol stent along the commissures and around the lower edges of the leaflet to create a valve. The valve was placed in a transparent tube and tested in a pulse duplicator. Physiologic pressures and flows were then applied to the valve for 30 cardiac cycles at 60 beats per minute. An endoscope and digital camcorder were used to capture valve performance in vitro. Simulated aortic and left ventricular pressures as well as fluid (water) flow rate were recorded.

Regurgitant fraction (RF) and effective orifice area  $A_{EO}$  were calculated as according to and compared with current standards (ISO 5840-1:2015) utilizing a custom Matlab (Mathworks, Natick, MA, USA) script. Effective orifice area was determined as the root mean square forward flow ( $q_v$ ; Equation (1)) divided by a constant value (51.6) times the square root of the mean pressure difference ( $\Delta p$ ), as measured over the positive pressure across the forward flow in mmHg, divided by the density ( $\rho$ ) of the test fluid in cm<sup>3</sup>. RF was calculated as the ratio of regurgitant volume (RV) divided by stroke volume (SV; Equation (3)). The valves were also exposed to fatigue testing on an accelerated wear tester (Durapulse, TA Instruments, New Castle, DE). Testing was performed at 37 °C in PBS solution and tested for an equivalent of 30 days in vivo.

Equations 1–3. Hydrodynamic calculations

$$q_{VRMS} = \sqrt{\frac{\int_{t_1}^{t_2} q_v(t)^2 dt}{t_2 - t_1}} \quad (1)$$

$$A_{EO} = \frac{q_{VRMS}}{51.6 \times \sqrt{\frac{\Delta p}{\rho}}} \quad (2)$$

$$RF = \frac{RV}{SV} \times 100 \quad (3)$$

## 2.8 | Statistical analysis

Analysis of the distribution of data, utilizing JMP statistical software (v. 10.0, SAS Institute Inc., Cary, NC, USA), from tensile tests illustrated that the data were non-parametric in nature. Consequently, a Kruskal–Wallis rank sum test with comparison using the Wilcoxon method was utilized. Biomechanical and porosity data were compared between the groups and considered significant for  $p < .05$ . Bioassay data were presented as median and interquartile range given the non-normality of distribution. Analysis of differences in collagen and GAG content between groups was performed using the non-parametric Kruskal–Wallis test. Bioassay data were compared against native cusps. A type I error rate of <.5 was considered statistically significant. All statistical

analyses were performed using JMP Pro 10 (SAS, North Carolina). ELISA data distribution was analysed utilizing MATLAB 2016a statistical toolbox (Mathworks, Natick, MA) using a one-way analysis of variance followed by a multi-comparison test. Data are presented as means  $\pm$  SD with statistical significance defined as  $p$  value  $<$  .05.

### 3 | RESULTS

#### 3.1 | Pericardial thickness

In the current study, the uniaxial mechanical properties of porcine pericardium that were native, decellularized, decell-sterilized, and fixed were compared with native cusps ( $n = 12$  each direction). For each group, pericardial thickness was assessed through digital caliper measurement at the centre of each individual sample (three thickness measurements were averaged). The collected native cusps were significantly thicker than all other groups ( $p < .0001$ ). Additionally, the decellularized and fixed groups were significantly thicker than the decellularized-sterilized ( $p = .0005$  and  $p = .0069$ , respectively) and native pericardium ( $p < .001$  and  $p = .0001$ , respectively); yet neither of these two latter groups were significantly different (Table 1).

#### 3.2 | Ultimate tensile strength

UTS was determined for each processing condition as the maximum stress before rupture, and the data demonstrated that tissue processing caused significant changes in the mechanical properties of the tissue (Figure 1). In both the circumferential direction, fixation ( $p = .0012$ ) and decell-sterilization ( $p = .0051$ ) caused significant declines in UTS relative to native pericardium. Even more extreme decreases were seen in the decellularized tissue. Although there were major declines in the UTS of the decellularized tissue ( $-81\%$ ,  $p < .001$ ), this value (Circ. 4.41 MPa) still remained over two times greater than the intrinsic circumferential UTS of native porcine valve leaflets (Circ. 1.32 MPa; Table 1). In the circumferential direction, there was a statistically

significant lower value of UTS found in the native valve cusps compared with all other groups, which could be attributed to increased thickness (Table 2). Calculation of stress accounts for thickness, and in this experiment, thickness varied significantly between conditions; therefore, the maximum tension of the tissues was evaluated to negate calculation errors from potential tissue swelling (Table 1).

#### 3.3 | Tensile stiffness

Utilizing the slope of load and displacement data, the overall stiffness of the tissue in each condition was evaluated. Native pericardium exhibited the highest value for stiffness closely followed by the fixed and decell-sterilized groups. Remarkably, there was a 76% decrease in stiffness, for the decellularized pericardium relative to the native pericardial tissue (Circ./Long.,  $p < .001$ ; Table 3). There was a statistically significant lower value of tensile stiffness found for the native valve cusps compared with all other groups.

#### 3.4 | ECM examination

##### 3.4.1 | SEM, Porosity, and TEM

Qualitative microstructure analysis of SEM images also confirmed that the superficial pore size was larger for the decellularized and decell-sterilized tissues (Figure 2i). Overall porosity, as determined by the liquid displacement method, of decellularized ( $\sim 87\%$ ) and decell-sterilized ( $\sim 79\%$ ) tissues was more similar to that of native cusps ( $\sim 77\%$ , Figure 2ii). As expected, native pericardial tissue was found to be statistically different than other groups ( $p = .05$ ), but more importantly, there was no significance found between decellularized and decell-sterilized pericardium relative to native cusps. Cross-sectional TEM images (Figure 3i) showed the collagen and elastin fibrils within the tissue specimens. Both the decellularized and decellularized and sterilized tissue specimens appeared to have mostly elastin at the surface, similar to the native cusps. Comparatively, the fixed and native pericardium seemed to have mostly collagen at the surface.

**TABLE 1** Ultimate tensile strength and thickness of processed pericardial tissue versus native tissues

Group	Ultimate tensile strength (MPa)				Tissue thickness (mm)			
	Circumferential		Longitudinal		Median	Interquartile range		
	Median	Interquartile range	Median	Interquartile range				
Decellularized	4.41	4.17–6.25	7.05	4.72–13.08	0.16	0.15–0.19		
Fixed	23.38	18.79–31.38	30.83	26.45–31.37	0.15	0.13–0.16		
Sterilized	19.62	11.55–24.24	26.26	19.4–31.97	0.12	0.09–0.14		
Native pericardium	27.55	24.5–45.74	44.41	41.48–64.34	0.10	0.08–0.12		
Native cusps	1.32	1.24–1.46	3.41	1.99–5.34	0.50	0.48–0.576		
Comparison	Z score		p value		Z score		p value	
Native cusps	Decellularized	2.62	.0089	3.94	<.0001	4.22	<.0001	
	Fixed		<.0001	4.11	<.0001	4.31	<.0001	
	Sterilized	4.22	<.0001	4.31	<.0001	–4.31	<.0001	
	Native pericardium	4.13	<.0001	4.22	<.0001	–4.23	<.0001	
Decellularized	Fixed	3.65	.0003	3.94	<.0001	–1.72	.0857	
	Sterilized	3.59	.0003	3.88	.0001	–3.46	.0005	
	Native pericardium	4.03	<.0001	4.03	<.0001	–4.08	<.0001	
Fixed	Sterilized	3.00	.5383	–1.51	.1320	–2.70	.0069	
	Native pericardium	3.24	.0012	1.45	.1481	–3.82	.0001	
Sterilized	Native pericardium	2.95	.0051	–2.53	.0114	1.94	0.0522	



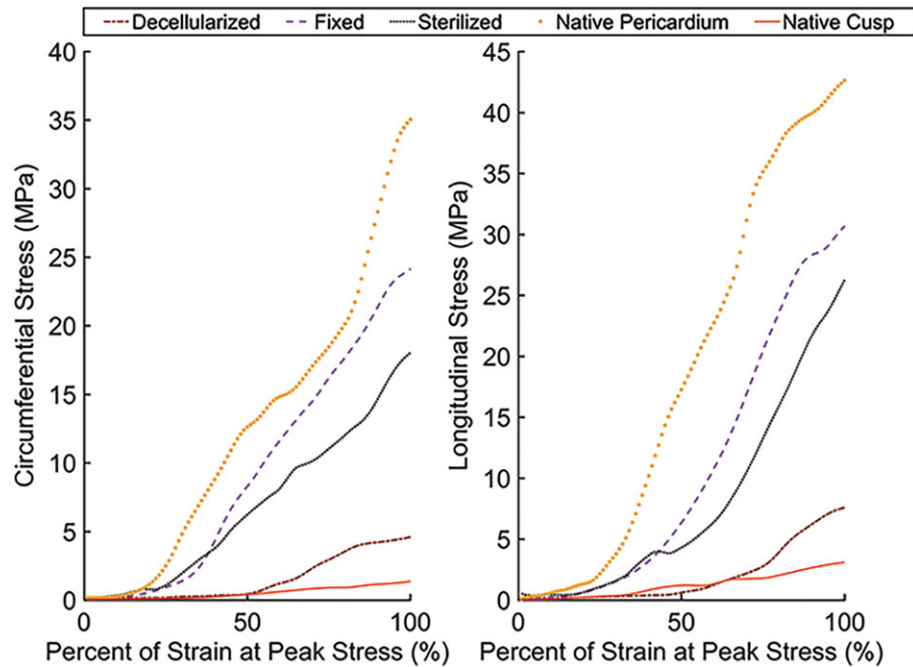


**FIGURE 1** Representative stress and strain in the (a) longitudinal and (b) circumferential directions for each group. Processing of porcine pericardial tissue generally showed a decrease in mechanical properties from the native pericardium, for the fixed, sterilized, and decellularized groups. Decellularization allowed for the pericardial tissue to be more mechanically representative of native valvular cusps compared with other processing conditions [Colour figure can be viewed at [wileyonlinelibrary.com](http://wileyonlinelibrary.com)]

**TABLE 2** Tension was calculated from uniaxial testing to evaluate properties sans tissue swelling

Group	Circumferential		Longitudinal		
	Median (N/m)	Interquartile range	Median (N/m)	Interquartile range	
Decellularized	0.87	0.62–1.01	1.41	0.74–1.69	
Fixed	3.62363	2.75–4.47	3.954	3.17–4.64	
Sterilized	1.686188	1.61–2.44	2.88575	1.76–3.44	
Native pericardium	2.893229	1.93–3.72	4.228059	3.72–4.9	
Native cusps	0.72915	0.56–0.8	1.645105	0.98–2.8	
Comparison		Z score	Z score	p value	Z score
Native cusps	Decellularized	0.92698	0.3539	–1.38478	.1661
	Fixed	4.11349	<.0001*	3.12759	.0018*
	Sterilized	4	<.0001*	1.5502	.1211
	Native pericardium	4.21626	<.0001*	3.26274	.0011*
Decellularized	Fixed	3.87424	.0001*	3.82381	.0001*
	Sterilized	3.53413	.0004*	2.78095	.0054*
	Native pericardium	3.97068	<.0001*	3.90912	<.0001*
Fixed	Sterilized	–3.24445	.0012*	–2.10256	.0355*
	Native pericardium	–1.01576	.3097	0.84325	.3991
Sterilized	Native pericardium	–3.07379	.0021*	–2.74737	.006*

### 3.5 | Biochemical assays

GAG and collagen content were extracted from the pericardial processed tissues and from native tissues for comparison (Figure 3ii). Native cusps had higher GAG content compared with the native pericardium and the processed tissues, where on average, native pericardium had 42% lower GAG content compared with native cusps. The average GAG content was  $0.14 \pm 0.01$ ,  $1.49 \pm 0.14$ ,  $0.13 \pm 0.02$ ,  $2.44 \pm 0.15$ , and  $5.69 \pm 0.37$   $\mu\text{g}/\text{mg}$  for decellularized, fixed, sterilized, native pericardium, and native cusps, respectively ( $p = .0015$ ).

Collagen content was significantly lower for native cusps compared with native pericardium and other pericardial processed groups

( $p = .0181$ ). The average collagen content was  $2.28 \pm 0.06$ ,  $2.24 \pm 0.05$ ,  $2.08 \pm 0.23$ ,  $2.62 \pm 0.9$ , and  $1.65 \pm 0.15$   $\mu\text{g}/\text{mg}$  for decellularized, fixed, sterilized, native pericardium, and native cusps, respectively. Microscopic TEM inspection also supported these findings showing more collagen microstructure in native pericardium compared with native cusps.

### 3.6 | Histology

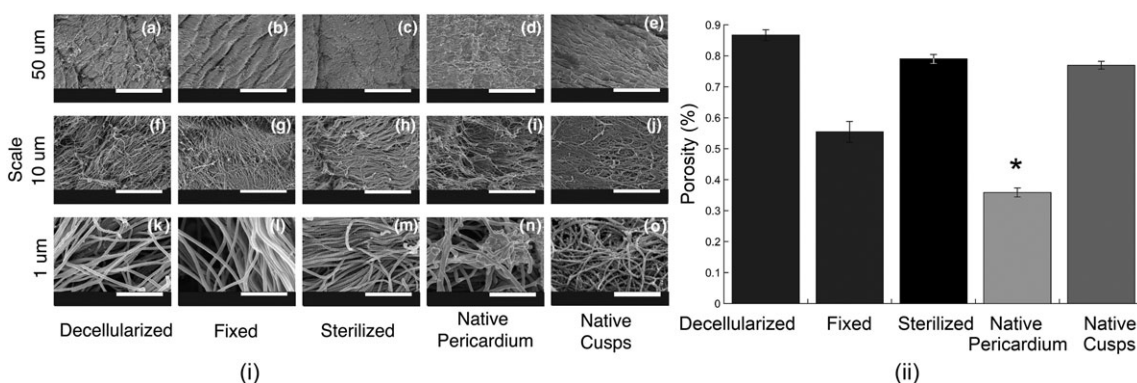
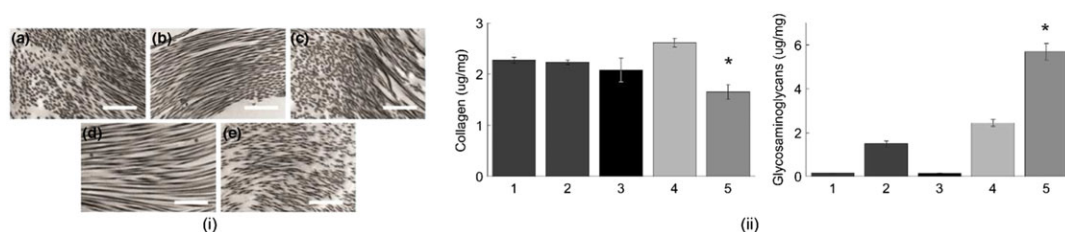
Residual cells were assayed through DAPI staining, and sections from tissues that underwent decellularization showed a notable lack of

**TABLE 3** Biomechanical stiffness of processed pericardium contrasted to native tissue

Group	Circumferential		Longitudinal	
	Median (MPa)	Interquartile range	Median (MPa)	Interquartile range
Decellularized	23.60	18.60–30.46	45.45	27.46–56.00
Fixed	100.38	81.33–128.51	158.7	131.95–197.57
Sterilized	44.86	33.8–77.17	63.04	36.36–81.53
Native pericardium	119.20	93.47–144.56	188.35	105.69–290.96
Native cusps	4.49	3.59–5.86	16.38	12.54–20.99

Comparison	Z score	p value	Z score	p value	
Native cusps	Decellularized	2.98	.0028*	4.11	<.0001*
	Fixed	4.22	<.0001*	4.11	<.0001*
	Sterilized	3.89	.0001*	4.31	<.0001*
	Native pericardium	4.13	<.0001*	4.22	<.0001*
Decellularized	Fixed	4.11	<.0001*	3.94	<.0001*
	Sterilized	1.80	.0725	3.13	.0018*
	Native pericardium	3.97	<.0001*	4.03	<.0001*
Fixed	Sterilized	-4.10	<.0001*	-3.07	.0021*
	Native pericardium	0.46	.6438	1.02	.3099
Sterilized	Native pericardium	-3.73	.0002*	-3.62	.0003*

**FIGURE 2** (i) Scanning electron micrographs for pericardial tissue that has been (a,f,k) decellularized in SDS, (b,g,l) fixed in glutaraldehyde, (c,h,m) sterilized by supercritical CO<sub>2</sub>, and native tissues including (d,i,n) fresh pericardium and (e,j,o) fresh leaflet cusps. Images were taken at magnifications of 1,000× (a–e), 5,000× (f–j), and 50,000× (k–o). (ii) Per cent porosity was determined for each group through the volume displacement method. \*Statistical significance ( $p < .05$ ) from all other groups**FIGURE 3** (i) Cross-sectional transmission electron microscopy images showing the collagen and elastin fibrils of (a) decellularized pericardium, (b) fixed pericardium, (c) sterilized pericardium, (d) native pericardium, and (e) native cusps. Scale bars: 1 μm. (ii) Bioassay results for the tissues showing median (a) collagen and (b) glycosaminoglycan production. 1 = Decellularized; 2 = decell-sterilized; 3 = fixed; 4 = native pericardium; 5 = native cusps. \*Statistical significance ( $p < 0.05$ ) from all other groups [Colour figure can be viewed at [wileyonlinelibrary.com](http://wileyonlinelibrary.com)]

nuclei labelled cells (Figure 4a–e). Haematoxylin and eosin, Masson's trichrome, and picosirius red staining illustrated relative maintenance of matrix, especially collagen, architecture, and alignment; however, tissue swelling was apparent in the decellularized and decell-sterilized tissues (Figure 4f–t). Finally, periodic acid–Schiff staining seemed to show relatively similar GAG amounts in the tissues as native pericardium but relatively less than native cusps (Figure 4u–y).

### 3.7 | Cell compatibility study

VECs and VICs were seeded onto the tissues and cultured for 30 days. Tissues, which had been decellularized and then sterilized, exhibited superficial colonization 30 days after initial cell seeding showing a lack of cytotoxicity in the tissue (Figure S1i). Furthermore, assaying of cell viability after 30 days showed colonies of cells with minimal red

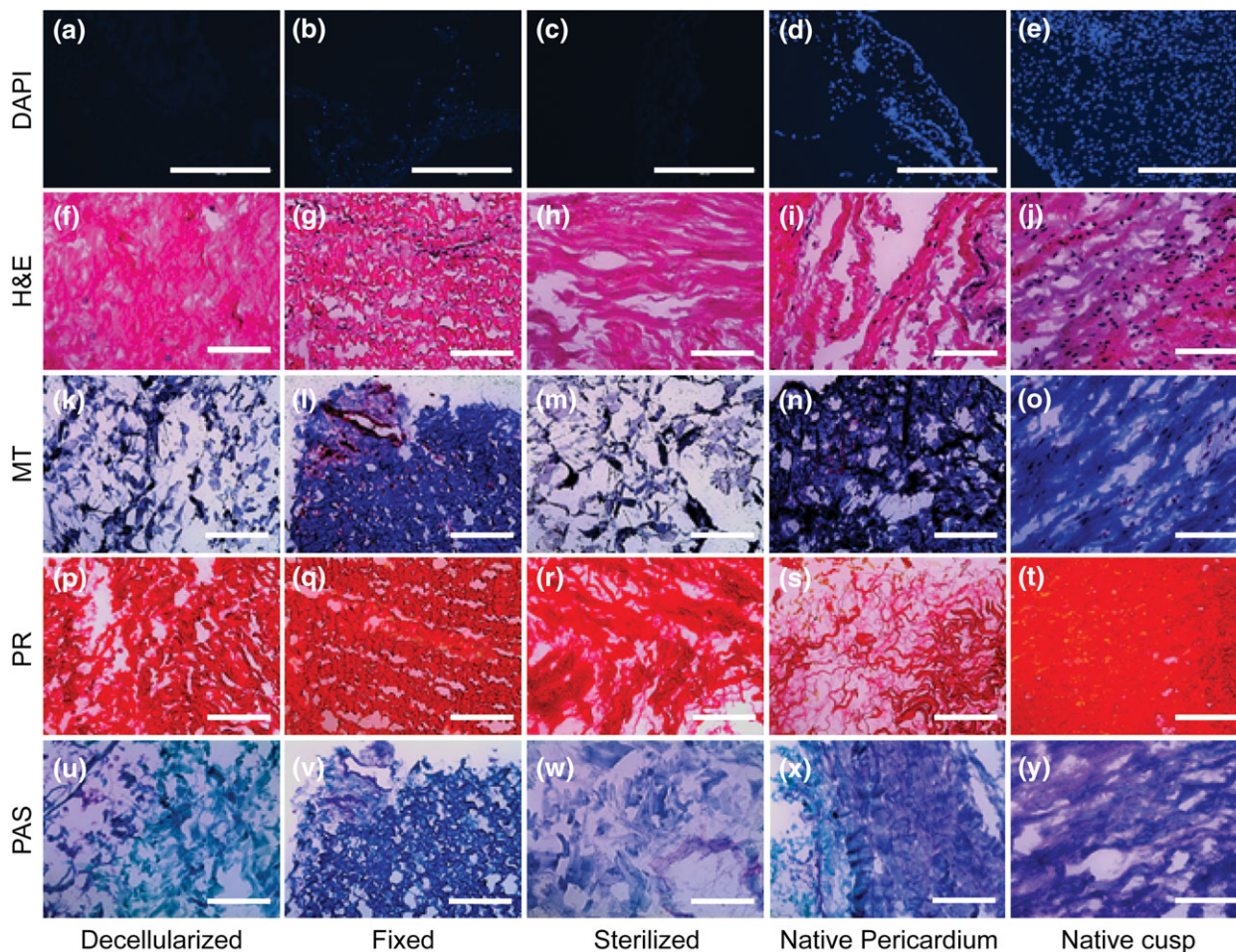


**FIGURE 4** Histological matrix characterization of decellularized, fixed, decell-sterilized, native pericardium, and native cusps. Sections were stained with (a–e) DAPI, (f–j) haematoxylin and eosin (H&E), (k–o) Masson's trichrome (MT), (p–t) picrosirius red (PR), and (u–y) alcian periodic acid–Schiff (PAS). Scale bars: DAPI = 400  $\mu$ m; H&E, MT, PR, and PAS = 200  $\mu$ m [Colour figure can be viewed at [wileyonlinelibrary.com](http://wileyonlinelibrary.com)]

labelled dead cells in all of the tissue processing conditions (Figure S1ii). The anti-alpha-gal staining was negative for the decellularized-sterilized porcine pericardial tissue (Figure S2). Although the decellularized-sterilized porcine pericardial process appeared to remove most the interstitial cellularity, alpha-gal persisted within the ECM on immunohistochemistry (Figure S2a–c). The quantification of the alpha-gal xenoantigen by ELISA analysis showed that there was a statistically significant difference for both native cusps ( $p = .0262$ ) and decellularized-sterilized pericardial ( $p = .0439$ ) when compared with native pericardial (Figure S2d).

### 3.8 | Suture retention

The mean suture retention strength for native cusp specimens was  $108.81 \pm 42.79$  g. As shown in Figure 5, this level was significantly exceeded by all other specimen types tested ( $p < .05$ ). Suture retention strength was more than doubled in the decellularized ( $205.51 \pm 83.14$  g) and sterilized tissues ( $315.13 \pm 98.12$  g), the latter which exceeded the strength even of native pericardium ( $289.55 \pm 96.20$  g); yet both groups exhibited significantly lower retention strength than the GA-fixed pericardium ( $477.15 \pm 106.69$  g;  $p < .0005$ , respectively).

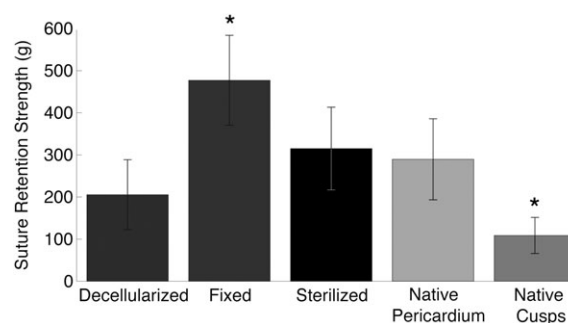


**FIGURE 5** Suture retention strength data for all tissue groups. \*Statistical significance ( $p < .05$ ) from all other groups

### 3.9 | Hydrodynamic evaluation

Hydrodynamic testing was performed on two prototype transcatheter valves made with decell and decell-sterilized pericardial tissue leaflets. In vivo aortic pressures were applied to the valve in a pulse duplicator system, and results showed that the tissue maintained integrity and suture retention under physiological pressures (Figure 6). The valves were within the range of  $A_{e0}$  standard of  $1.00 \text{ cm}^3$  (Figure 6ii,a). Additionally, there was little regurgitation ( $<6\%$ ), which was well within standard ISO 5840, which requires



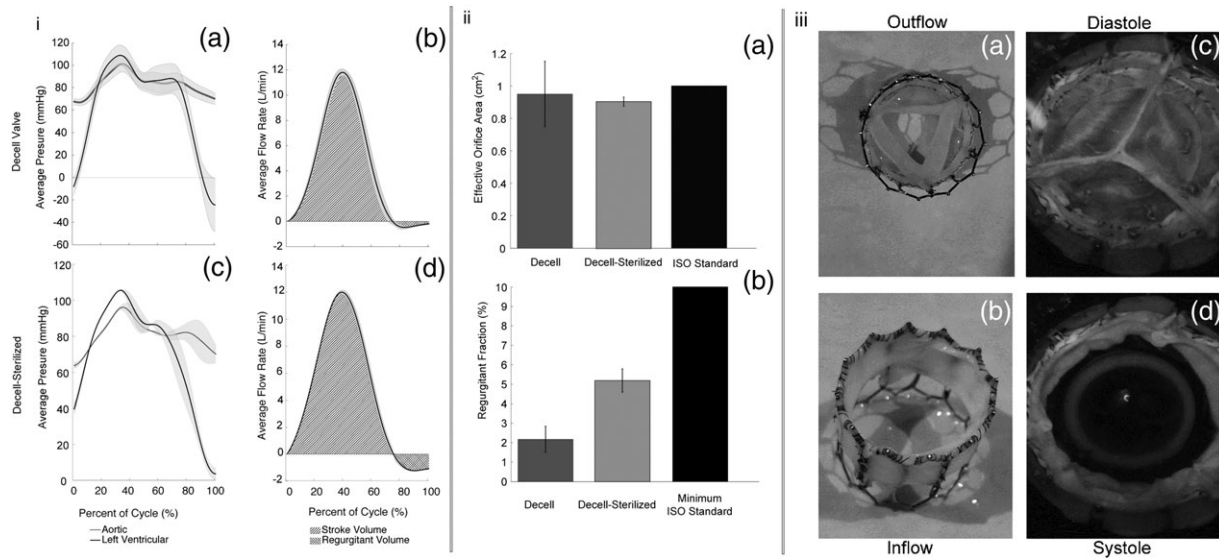


**FIGURE 6** (i) Hydrodynamic testing: Pressure and flow wave forms for (a–b) transcatheter heart valve prototype with decellularized porcine pericardial tissue leaflets, (c–d) transcatheter heart valve prototype with decell-sterilized porcine pericardial tissue leaflets. (ii) Valve calculations referenced against ISO standards: (a) effective orifice area was within ISO standards ( $\sim 1.00 \text{ cm}^2$ ); (b) low regurgitant fraction was seen for both valves ( $< 10\%$ ). (iii) (a–b) Bird's eye and side view of a prototype transcatheter aortic valve. (c–d) Hydrodynamic testing of a decellularized valve under physiological conditions: (c) diastole and (d) systole

$< 10\%$  RF (Figure 6ii,b; ISO 5840-1:2015). The valves were subjected to accelerated wear testing and successfully met 30 days *in vivo* ( $\sim 3,330,000$  cycles), which should provide adequate time for the recellularization process to begin.

## 4 | DISCUSSION

Pericardial tissue is easily accessible and is structurally and functionally similar to human tissue, and decellularization has revolutionized the field in allowing for non-immunogenic tissues to be produced (Bourgine et al., 2013; Crapo et al., 2011). Still, the issue of mechanical durability and biological viability, especially in regard to immunogenicity, has come into question when utilizing fixed or decellularized tissues (Bourgine et al., 2013). Recent works have focused on investigating the utility of decellularized pericardial tissues for crafting aortic heart valves as they are highly biocompatible and are capable of remodelling and growing (Gauvin et al., 2012). Sterilization is an important step in preparation of TEHV for *in vivo* utilization, and in this study, the impact of an idealized sterilization process on decellularized porcine pericardial, through commercial  $s\text{CO}_2$ , as previously optimized, was explored. It was hypothesized that these tissues would show more similar mechanical, structural, and appropriate cell viability, relative to native valvular tissue.

In this study, the uniaxial tensile properties of porcine pericardial tissue were evaluated. Samples ( $n = 12$  each) included native, fixed, decellularized, and decellularized then sterilized pericardium, as well as fresh native valvular cusps. Our processed pericardial tissues, with the exception of the fixed condition, generally showed significant decreases in UTS but still retained properties greater than valvular tissues (Figure S3). Reduced collagen and greater GAG levels in the

native cusps, as determined by bioassays and TEM, likely account for the differences seen in reference to the pericardial groups (Figure 3). These findings match similar testing done in bovine pericardium that showed that the UTS of native and fixed pericardium was over 50% stronger than native cusps (Arbeiter, Grabow, Wessargues, Sternberg, & Schmitz, 2012). Additionally, our decellularized tissues showed similar UTS to those reported (Morticelli, Korossis, Thomas, Roberts, & Ingham, 2013); yet we observed anisotropy in our material as is seen in other published literature (Gauvin et al., 2012; Labrosse et al., 2016). Our results show that the decellularization process lowers the GAGs compared with the native scaffolds (Figure 3), likely due to the caustic nature of SDS. Current research shows that many ECM proteins are glycosylated, which in turn affects protein folding, solubility, binding, and degradation (Barallobre-Barreiro, Baig, Fava, Yin, & Mayr, 2017). Potentially reducing the concentration of SDS would allow the GAG content to be more representative of native cusps. However, the lower GAG content observed on our tissue still allowed VICs to attach and proliferate. The decellularized group became more characteristic of native valvular cusps in both planar axes, which was further demonstrated when disregarding the effects of tissue thickness, but still retained mechanical properties that could help to mitigate the effects of inevitable degradation *in vitro* or *in vivo*. However, there were some discrepancies between the UTS and tension values among some tissue groups. The native valve cusps did not have a significantly lower tension compared with the longitudinal sterilized group, whereas they showed significantly lower UTS compared with the same group; the fixed group had significantly higher tension compared with the sterilized group, whereas they did not show any difference in terms of UTS. These findings suggest that tissue thickness, which can be highly variable due to tissue swelling with decellularization (Xu et al., 2014), may give erroneous results in

tension calculations that may not be representative of the true mechanical properties of the tissues.

In terms of stiffness, a similar trend was observed as compared with the changes in UTS. Our fixed pericardium showed similar stiffness to other fixed porcine pericardial tissues that have been tested (average of planar axes ~150 MPa) and is much less stiff than fixed bovine pericardium (~250 MPa; Gauvin et al., 2012). Similar to the results of UTS testing, sterilization had a restorative effect on the elastic properties of the tissue.

Although decellularization shifted the mechanical properties of the affected pericardium towards those of the native valvular cusps, sterilization had a moderate effect in the opposing direction. Although the major method of sterilization, via sCO<sub>2</sub>, has been reported to not have a cross-linking effect on biomaterials (Bernhardt et al., 2015; Hennessy et al., 2017), interesting compressive and tensile increases post-treatment have been noted in studies utilizing this technique, as well as in the data at hand. Bernhardt et al. (2015) postulated that the high pressure utilized with sCO<sub>2</sub> sterilization may impact biomaterial nanostructure in unexpected manners. In the current study, no obvious changes in structure between the decellularized and sterilized groups were observed. However, chemicals used by the vendor to prepare the tissue, such as custom reagents, could have minor cross-linking abilities that may be explanatory of the contrast in mechanics. Regardless, the stiffness of the sterilized pericardial tissue still showed significant decreases in mechanics, which may be of importance for physiological application of the tissue.

The aortic valve has evolved to efficiently handle the stretch and strain on the cusps with progressive openings and closures (Simmons, 2009). Valvular cells have become specially adapted to this environment and respond favourably to specific levels of elasticity in the matrix. Too stiff or elastic of a tissue may promote overt fibrosis, detachment, or even apoptosis (Wyss et al., 2012). It is possible that current bioprosthetic valve dysfunction and calcification in bovine pericardial valves result from inadequate consideration of cell phenotype (Simionescu, 2004). Collatusso et al. (2011) demonstrated that decellularized bovine pericardial valves showed no calcification 180 days post-implantation in an ovine model relative to the clinical standard, GA-fixed valves (Santoro et al., 2016).

This study has demonstrated that decellularized and decell-sterilized porcine pericardial tissue exhibits improved elasticity (Long. Median 23.13 MPa), similar to reported human pericardial stiffness (20.19 MPa; Lee & Boughner, 1985). There is potential that declines in the mechanical properties of the pericardium could be indicative of significant matrix disruption. Alterations in the microscopic structure of the ECM of the pericardium are likely responsible for this shift. Qualitative inspection of SEM micrographs demonstrates some degree of ECM disruption in the decellularized group but similar if not more extreme effects were seen in the fixed group (Figure 3). However, general perseveration of histological matrix components was seen, and in this study, sterilization improved the mechanical properties of the decellularized tissue potentially through partial fixation by molecular cross-linking. This would imply that decellularization causes degradation of intermolecular connections and might be the fundamental cause of increases in elasticity and

decreases in tensile strength. Yet there is potential that such disruption may have biological implications, such as increased thrombus formation, that will be investigated in future studies.

The tissue tested demonstrated superior suture retention to native cusps (Figure 5). Furthermore, hydrodynamic and accelerated wear testing illustrated that competent and mechanically tough valve prototypes were created. However, there is potential that the material may be primed for enzymatic degradation that was not explored in this study. Increased degradation could also be favourable for cell infiltration and remodelling and used to a manipulative advantage, if the temporal-spatial aspects of this component are well defined, augmented, and optimized. Overall, decellularization and sterilization trends towards shifting the mechanical properties, from UTS to stiffness, to more closely resemble the mechanical properties of a native porcine valve (Figure 1), which could potentially allow this material to be superior to current dogmas in terms of cellular favorability.

Valvular interstitial and endothelial cells were seeded *in vitro* gravimetrically. SEM of the surface of the pericardial tissue and the cell viability assay have helped to demonstrate that the tissue utilized was a suitable substrate for both cell types as cell seeding occurred matching the results of other studies (Figure S1; Santoro et al., 2016). Lanuti et al. (2015) was able to show re-endothelialization of a heart valve scaffold, and likewise, in this study, endothelial cells were colonized on the surface of the tissue. As these cells exist *in vivo* as a superficial monolayer, they may be beneficial in enhancing construct performance. Other studies have shown that decellularization, as performed with SDS, of porcine valve leaflets resulted in a dense matrix with relatively small pores (Liao, Joyce, & Sacks, 2008). It was postulated that recellularization of the matrix may be difficult as cells would have difficulty invading the space. Similarly, in the current study, the porosity of decellularized tissues were no different than native cusps. Alternative techniques such as injection of cells into the matrix could be useful in promoting recellularization (Vincentelli et al., 2007); yet residual SDS may lead to cytotoxicity *in vivo* that could limit cell growth and expansion.

Alpha-gal, a marker of immunogenicity, was sparsely observed in the sterilized pericardial tissue (Figure S2). There have been conflicting reports in literature on the impact of alpha-gal since studies showed that the alpha-gal antigen appeared in bovine and porcine commercially available valves (Naso, Gandaglia, Lop, Spina, & Gerosa, 2011). Interestingly, xenografts with alpha-gal used in a non-human primate model showed that the ECM elicits a serum antibody response, but no adverse effects occurred with tissue remodelling (Daly et al., 2009). Future primate animal studies will confirm if additional tissue processing steps of the xenograft with alpha-galactosidase is necessary. Konakci et al. (2005) showed alpha-galactosidase processing further mitigated the immune response against the bioprostheses and extended durability.

The creation for a sterilized, off-the-shelf, valve allows for veritably unlimited possibilities for cell integration, as this work can easily be done prior to implantation or can be bypassed completely. Previously, this laboratory has shown success in recellularizing acellular porcine aortic valves *in vivo*, but a combination of *in vitro*

cell seeding and in vivo recellularization may be ideal for the introduction of autologous cell into the tissue (Hennessy et al., 2017). Thus, in the future, optimal cell seeding procedures will need to be defined, and in vivo studies will be necessary to determine effective spatial and temporal aspects of recellularization of this biomaterial.

Besides the optimization of cell–biomaterial interactions, there are several limitations for this biomaterial and TEHV in general moving forward. There are concerns regarding the integrity of decellularized tissue due to matrix disruption; yet potential cell infiltration could allow for native or autologous cells to strengthen and remodel the existing matrix. Moreover, the comparatively strong mechanical properties of pericardial tissue shown in this study could allow it to be a potential target for valvular applications, despite matrix disruption. Proper cell viability and function must be determined to ensure the tissue is capable of normal repair and remodelling (Sacks, Schoen, & Mayer, 2009). Although alpha-gal was minimally observed in the sterilized tissue of this study, there is potential that other residual antigens in the tissue remain, as have been reported in acellular whole porcine valves (Simon et al., 2003). Future studies utilizing the current technique and additional stepwise antigen solubilization steps (Wong & Griffiths, 2014) or transgenic enzymes or bacterium that target specific epitopes could ensure the safety of this implant for clinical applications (Nam et al., 2012). These factors, and more, all need to be fully grasped before decellularized pericardium is a feasible material for human application.

Although such bioprosthetic valves are likely achievable in vitro, complex manufacturing conditions, such as the necessity of perfusion following cell seeding, and preconditioning to physiological conditions may be a limiting step in mass production; however, in non-emergency situations, these sterile valves could be made on a for-demand basis thus allowing them to be practical and cost-effective to a manufacturer. The investigation of commercial sterilization has allowed for the potential for off-the-shelf tissues to be produced and maintained; yet longitudinal degradation studies need to be performed to validate long-term tissue integrity. As we better understand how to manipulate the mechanical properties of pericardium, bioprosthetic geometry, and cell integration, there is great potential for a viable and operative pericardial heart valve to be produced. Therefore, future work in our laboratory will focus on animal studies to assess the in vivo performance of pericardial valves.

## 5 | CONCLUSION

Utilization of tissue engineering paradigms to make xenogeneic tissue suitable for transplant has great potential. Investigations of compatible substance necessitate that the biomaterial be mechanically stable, functionally sound, biocompatible, non-immunogenic, and capable of supporting cell-mediated growth, repair, and remodelling. In this study, we compared decellularized, fixed, and decell-sterilized pericardium relative to native valvular and pericardial tissue in order to assess the impact of processing, especially sterilization, on the material's mechanical properties. The decellularized tissue, although showing lower mechanical properties than the other treatments, still

demonstrated elastic properties more similar to the average porcine aortic cusp that was mostly preserved in the sterilized group. Furthermore, decell-sterilized tissue has the advantage of being able to accept host-derived cells, allowing for surface endothelialization, as well as a lack of native immunoglobulins, and a sterile environment for long-term structural stability. Future work will focus on studying in vivo degradation, performance, and recellularization of decell-sterilized pericardial valves as well as characterizing residual antigenicity. Overall, decellularized porcine pericardial tissue holds promise for its application in the creation of tissue-engineered valves.

## ACKNOWLEDGEMENTS

This work has been supported by the HH Sheikh Hamed bin Zayed Al Nahyan Program in Biological Valve Engineering. This research was supported in part by the National Institute of Health T32 (HL007111) training grant in cardiovascular. The authors would like to thank Ahna E. Buntrock for tissue testing assistance, as well as Scott Gamb and the Microscopy and Cell Analysis Core at the Mayo Clinic for their work in producing SEM images.

## CONFLICT OF INTEREST

The authors have declared that there is no conflict of interest.

## ORCID

Joshua A. Choe  <http://orcid.org/0000-0003-4757-8849>

Melissa D. Young  <http://orcid.org/0000-0002-6519-4999>

## REFERENCES

- ANSI/AAMI/ISO 7198:2016. (2016). Cardiovascular implants and extracorporeal systems—Vascular prostheses—Tubular vascular grafts and vascular patches tubular vascular prostheses, Section, A.5.7: Suture retention strength.
- Arbeiter, D., Grabow, N., Wessarges, Y., Sternberg, K., & Schmitz, K.-P. (2012). Suitability of porcine pericardial tissue for heart valve engineering: biomechanical properties. *Biomedizinische Technik*, 57(Suppl. 1), 882–883.
- ASTMF2150–13. (n.d.) Standard guide for characterization and testing of biomaterial scaffolds used in tissue-engineered medical products.
- Barallobre-Barreiro, J., Baig, F., Fava, M., Yin, X., & Mayr, M. (2017). Glycoproteomics of the extracellular matrix: a method for intact glycopeptide analysis using mass spectrometry. *Journal of Visualized Experiments : JoVE*, 122, 55674. <https://doi.org/10.3791/55674>
- Bernhardt, A., Wehrl, M., Paul, B., Hochmuth, T., Schumacher, M., Schütz, K., & Gelinsky, M. (2015). Improved sterilization of sensitive biomaterials with super critical carbon dioxide at low temperature. *PLoS One*, 10(6), 1–19.
- Bourgine, P. E., Pippenger, B. E., Todorov, A. Jr., Tchang, L., & Martin, I. (2013). Tissue decellularization by activation of programmed cell death. *Biomaterials*, 34(26), 6099–6108.
- Braga-Vilela, A. S., Pimentel, E. R., Marangoni, S., Toyama, M. H., & de Campos Vidal, B. (2008). Extracellular matrix of porcine pericardium: Biochemistry and collagen architecture. *The Journal of Membrane Biology*, 221(1), 15–25.
- Butcher, J. T., Simmons, C. A., & Warnock, J. N. (2008). Mechanobiology of the aortic heart valve. *The Journal of Heart Valve Disease*, 17(1), 62–73.
- Collatusso, C., Affonso da Costa, F. D., Roderjan, J. G., Vieira, E. D., Myague, N. I., & de Noronha, L. (2011). Decellularization as an

- anticalcification method in stentless bovine pericardium valve prosthesis: A study in sheep. *Revista Brasileira de Cirurgia Cardiovascular*, 26(3), 419–426.
- Crapo, P. M., Gilbert, T. W., & Badylak, S. F. (2011). An overview of tissue and whole organ decellularization processes. *Biomaterials*, 32(12), 3233–3243.
- Daly, K., Stewart-Akers, A. M., Hara, H., Ezzelarab, M., Long, C., Cordero, K., ... Badylak, S. F. (2009). Effect of the  $\alpha$ Gal epitope on the response to small intestinal submucosa extracellular matrix in a nonhuman primate model. *Tissue Engineering Parts A*, 15(12), 3877–3888. <https://doi.org/10.1089/ten.tea.2009.0089>
- d'Arcy, J. L., Prendergast, B. D., Chambers, J. B., Ray, S. G., & Bridgewater, B. (2011). Valvular heart disease: The next cardiac epidemic. *Heart (British Cardiac Society)*, 97(2), 91–93.
- Easterbrook, C., & Maddern, G. (2008). Porcine and bovine surgical products: Jewish, Muslim, and Hindu perspectives. *Archives of Surgery*, 143(4), 366–370. discussion 370
- Fentie, I. H., Allen, D. J., Schenck, M. H., & Didio, L. J. (1986). Comparative electron microscopic study of bovine, porcine and human parietal pericardium, as materials for cardiac valve bioprostheses. *Journal of Submicroscopic Cytology*, 18(1), 53–65.
- Gauvin, R., Marinov, G., Mehri, Y., Klein, J., Li, B., Larouche, D., ... Guidoin, R. (2012). A comparative study of bovine and porcine pericardium to highlight their potential advantages to manufacture percutaneous cardiovascular implants. *Journal of Biomaterials Applications*, 28(4), 552–565.
- Grunkemeier, G. L., Furnary, A. P., Wu, Y., Wang, L., & Starr, A. (2012). Durability of pericardial versus porcine bio-prosthetic heart valves. *The Journal of Thoracic and Cardiovascular Surgery*, 144(6), 1381–1386.
- Hasan, A., Ragaert, K., Swieszkowski, W., Selimović, Š., Paul, A., Camci-Unal, G., ... Khademhosseini, A. (2014). Biomechanical properties of native and tissue engineered heart valve constructs. *Journal of Biomechanics*, 47(9), 1949–1963.
- Hennessy, R. S., Lerman, A., Jana, S., Tefft, B. J., Helder, M. R., Young, M. D., ... Stoyles, N. J. (2017). Supercritical carbon dioxide-based sterilization of decellularized heart valves. *JACC: Basic to Translational Science*, 2(1), 71–84.
- Hulsmann, J., Grun, K., El Amouri, S., Barth, M., Hornung, K., Holzfuß, C., ... Akhyari, P. (2012). Transplantation material bovine pericardium: Biomechanical and immunogenic characteristics after decellularization vs. glutaraldehyde-fixing. *Xenotransplantation*, 19(5), 286–297.
- ISO 5840-1:2015. (2015). (E): Cardiovascular implants: cardiac valve prostheses. Part 1: General requirements. Geneva: ISO Copyright Office; 56.
- Jang, W., Choi, S., Kim, S. H., Yoon, E., Lim, H. G., & Kim, Y. J. (2012). A comparative study on mechanical and biochemical properties of bovine pericardium after single or double crosslinking treatment. *Korean Circulation Journal*, 42(3), 154–163.
- Kasimir, M. T., Rieder, E., Seebacher, G., Nigisch, A., Dekan, B., Wolner, E., ... Simon, P. (2006). Decellularization does not eliminate thrombogenicity and inflammatory stimulation in tissue-engineered porcine heart valves. *The Journal of Heart Valve Disease*, 15(2), 278–286.
- Konacki, K. Z., Bohle, B., Blumer, R., Hoetzenecker, W., Roth, G., Moser, B., ... Ankersmit, H. J. (2005). Alpha-gal on bioprostheses: Xenograft immune response in cardiac surgery. *European Journal of Clinical Investigation*, 35(1), 17–23.
- Labrosse, M. R., Jafar, R., Ngu, J., & Boodhwani, M. (2016). Planar biaxial testing of heart valve cusp replacement biomaterials: Experiments, theory and material constants. *Acta Biomaterialia*, 45, 303–320.
- Lanuti, P., Serafini, F., Pierdomenico, L., Simeone, P., Bologna, G., Ercolino, E., ... Miscia, S. (2015). Human mesenchymal stem cells reendothelialize porcine heart valve scaffolds: Novel perspectives in heart valve tissue engineering. *Biores Open Access*, 4(1), 288–297.
- Lee, J. M., & Boughner, D. R. (1985). Mechanical properties of human pericardium. Differences in viscoelastic response when compared with canine pericardium. *Circulation Research*, 57(3), 475–481.
- Liao, J., Joyce, E. M., & Sacks, M. S. (2008). Effects of decellularization on the mechanical and structural properties of the porcine aortic valve leaflet. *Biomaterials*, 29(8), 1065–1074.
- Loh, Q. L., & Choong, C. (2013). Three-dimensional scaffolds for tissue engineering applications: Role of porosity and pore size. *Tissue Engineering. Part B, Reviews*, 19(6), 485–502.
- Martin, C., & Sun, W. (2012). Biomechanical characterization of aortic valve tissue in humans and common animal models. *Journal of Biomedical Materials Research. Part A*, 100(6), 1591–1599.
- Mendoza-Novelo, B., Avila, E. E., Cauich-Rodriguez, J. V., Jorge-Herrero, E., Rojo, F. J., Guinea, G. V., & Mata-Mata, J. L. (2011). Decellularization of pericardial tissue and its impact on tensile viscoelasticity and glycosaminoglycan content. *Acta Biomaterialia*, 7(3), 1241–1248.
- Morticelli, L., Korossis, S., Thomas, D., Roberts, N., & Ingham, E. (2013). Investigation of the suitability of decellularized porcine pericardium in mitral valve reconstruction. *The Journal of Heart Valve Disease*, 22(3), 1–14.
- Nam, J., Yong, J. K., Choi, S.-Y., Sung, S.-C., Lim, H.-G., Park, S.-s., & Kim, S.-H. (2012). Changes of the structural and biomechanical properties of bovine pericardium after the removal of  $\alpha$ -gal epitopes by decellularization and  $\alpha$ -galactosidase treatment. *Korean J Thorac Cardiovasc Surg*, 45, 380–389.
- Naso, F., Gandaglia, A., Lop, L., Spina, M., & Gerosa, G. (2011). First quantitative assay of alpha-gal in soft tissues: Presence and distribution of the epitope before and after cell removal from xenogeneic heart valves. *Acta Biomaterialia*, 7, 1728–1734.
- Sacks, M. S., Schoen, F. J., & Mayer, J. E. (2009). Bioengineering challenges for heart valve tissue engineering. *Annual Review of Biomedical Engineering*, 11, 289–313.
- Santoro, R., Consolo, F., Spiccia, M., Piola, M., Kassem, S., Prandi, F., ... Pesce, M. (2016). Feasibility of pig and human-derived aortic valve interstitial cells seeding on fixative-free decellularized animal pericardium. *Journal of Biomedical Materials Research Part B, Applied Biomaterials*, 104(2), 345–356.
- Schmidt, C. E., & Baier, J. M. (2000). Acellular vascular tissues: Natural biomaterials for tissue repair and tissue engineering. *Biomaterials*, 21(22), 2215–2231.
- Simionescu, D. T. (2004). Prevention of calcification in bio-prosthetic heart valves: Challenges and perspectives. *Expert Opinion Biological Therapies*, 4, 1971–1985.
- Simmons, C. A. (2009). Aortic valve mechanics: An emerging role for the endothelium. *Journal of the American College of Cardiology*, 53(16), 1456–1458.
- Simon, P., Kasimir, M. T., Seebacher, G., Weigel, G., Ullrich, R., Salzer-Muhar, U., ... Wolner, E. (2003). Early failure of the tissue engineered porcine heart valve SYNERGRAFT in pediatric patients. *European Journal of Cardio-Thoracic Surgery*, 23(6), 1002–1006.
- Steinbock, G., Stock, U., Karim, N., Mertsching, H., Timke, A., Meliss, R. R., ... Bader, A. (2000). Tissue engineering of pulmonary heart valves on allogenic acellular matrix conduits: In vivo restoration of valve tissue. *Circulation*, 102(19 Suppl 3), III-50–III-55.
- Thubrikar, M., Piepgrass, W. C., Bosher, L. P., & Nolan, S. P. (1980). The elastic modulus of canine aortic valve leaflets in vivo and in vitro. *Circulation Research*, 47(5), 792–800.
- Vincentelli, A., Wautot, F., Juthier, F., Fouquet, O., Corseaux, D., Marechaux, S., ... Jude, B. (2007). In vivo autologous recellularization of a tissue-engineered heart valve: Are bone marrow mesenchymal stem cells the best candidates? *The Journal of Thoracic and Cardiovascular Surgery*, 134(2), 424–432.
- Voges, I., Bräsen, J. H., Entenmann, A., Scheid, M., Scheewe, J., Fischer, G., ... Rickers, C. (2013). Adverse results of a decellularized tissue-



- engineered pulmonary valve in humans assessed with magnetic resonance imaging. *European Journal of Cardio-Thoracic Surgery*, 44(4), e272–e279.
- Walther, T., Blumenstein, J., van Linden, A., & Kempfert, J. (2012). Contemporary management of aortic stenosis: Surgical aortic valve replacement remains the gold standard. *Heart (British Cardiac Society)*, 98(Suppl 4), iv23–iv29.
- Wilson, G. J., Courtman, D. W., Klement, P., Lee, J. M., & Yeger, H. (1995). Acellular matrix: A biomaterials approach for coronary artery bypass and heart valve replacement. *The Annals of Thoracic Surgery*, 60(2 Suppl), S353–S358.
- Wong, M. L., & Griffiths, L. G. (2014). Immunogenicity in xenogeneic scaffold generation: Antigen removal versus decellularization. *Acta Biomaterialia*, 10(5), 1806–1816.
- Wyss, K., Yip, C. Y., Mirzaei, Z., Jin, X., Chen, J. H., & Simmons, C. A. (2012). The elastic properties of valve interstitial cells undergoing pathological differentiation. *Journal of Biomechanics*, 45(5), 882–887.
- Xu, H., Xu, B., Yang, Q., Li, X., Ma, X., Xia, Q., ... Zhang, Y. (2014). Comparison of decellularization protocols for preparing a decellularized porcine annulus fibrosus scaffold. *PLoS One*, 9(1), e86723.

## SUPPORTING INFORMATION

Additional supporting information may be found online in the Supporting Information section at the end of the article.

Data S1 Supporting info item

**How to cite this article:** Choe JA, Jana S, Tefft BJ, et al. Bio-material characterization of off-the-shelf decellularized porcine pericardial tissue for use in prosthetic valvular applications. *J Tissue Eng Regen Med*. 2018;12:1608–1620. <https://doi.org/10.1002/term.2686>